



Electrochemical behaviour of a novel alloy steel in alkali-activated slag mortars

Jinjie Shi*, Jing Ming, Wei Sun

Jiangsu Key Laboratory of Construction Materials, School of Materials Science and Engineering, Southeast University, Nanjing, 211189, China



ARTICLE INFO

Keywords:

Alkali-activated slag
Alloy steel
Mortar
Corrosion resistance
Corrosion products

ABSTRACT

The present paper aims to investigate the passivation capability and accelerated chloride-induced corrosion behaviour of a novel alloy steel (00Cr10MoV) and a conventional low-carbon steel (20MnSiV) in ordinary Portland cement (OPC) and alkali-activated slag (AAS) mortars. Both steels were embedded in mortars with intact mill scale. Compared with OPC mortar, AAS mortar resulted in the formation of less protective passive film for both 20MnSiV and 00Cr10MoV steels after passivation due to the presence of reducing sulphides. Despite this, the initial negative effect of AAS mortar on 20MnSiV steel can be well compensated by its denser interfacial microstructure after the occurrence of active corrosion induced by chlorides. As for 00Cr10MoV steel in AAS mortar, however, this compensating effect was less pronounced. Moreover, unexpected low passivation capability and corrosion resistance can be confirmed for 00Cr10MoV steel in both OPC and AAS mortars due to the presence of defective and Cr-depleted mill scale.

1. Introduction

Nowadays, sustainability is becoming a very important factor in the design of reinforced concrete structures (RCSs) [1–3]. One strategy being used is the replacement of conventional Portland cement with some low-carbon materials (industrial by-products, such as slag and fly ash, etc.) from the point of view of energy conservation and emission reduction [2,4–6]. In addition, improved sustainability can also be achieved by prolonging the service life of RCSs using corrosion-resistant steels [2,7].

It is well known that alkali-activated materials (AAMs), as one type of low-carbon materials, have been investigated extensively for their hydration reactions, volumetric deformation and carbonation process, etc. [4–6,8–12]. Yet, relatively few studies have been carried out concerning the steel corrosion related durability performance in AAMs and more importantly, the corrosion mechanism of steels in AAMs is not clear so far [13–20]. It was reported that the passivation capability of steel in alkali-activated fly ash (AAFA) mortars was similar with ordinary Portland cement (OPC) mortars and the passive state stability was dependent upon the type of activator [21]. Moreover, in the presence of chlorides, AAFA mortars/concretes provided better corrosion protection to embedded steels than the specimens manufactured by OPC for a variety of reasons [13,16–18]. When simultaneously subjected to carbonation, however, AAFA mortars afforded a lower corrosion protection to embedded steels compared with OPC mortars

though a limited chloride content was detected in AAFA mortars [19].

The passivation mechanism and corrosion performance of steels in alkali-activated slag (AAS) materials are very complex due to the presence of sulphides in slag [14,22–28]. It was confirmed that sulphides in the pore solution of AAS would inhibit the spontaneous formation of protective passive film [23,26,27]. In addition, the other main challenge for AAS (also for AAFA) materials is the decreasing pH value on the steel surface due to the ion exchange (alkali loss) [14,29] and continuous carbonation [19,25] after long-term exposure to severe environments, which may finally result in the lower corrosion resistance of steels compared with OPC materials.

In recent decades, stainless steels have been used as one type of corrosion-resistant steels in marine construction [7,17,30–33]. Although traditional 304 and 316 stainless steels have superior corrosion resistance in severe environments, their high price due to the addition of expensive alloying elements and the potential pollution during pickling process for removing the mill scale limits their widespread application in RCSs [7,32,34–36]. Therefore, several types of low-Ni stainless steels and duplex stainless steels have been developed for possible application in RCSs [17,18,31,37].

In addition, Cr-bearing alloy steels, which are more economical compared with traditional stainless steels, have also drawn great attention over the last decades [38–53]. It was confirmed that a stable passive film was naturally formed for alloy steels containing high Cr content in concrete [39,41,46,47,50]. Yet, for alloy steels with low Cr

* Corresponding author.

E-mail address: jinjies@seu.edu.cn (J. Shi).

Table 1
Chemical compositions of investigated steels (wt.%).

Steel	Chemical compositions									
	Fe	C	Si	Mn	P	S	V	Cr	Mo	
20MnSiV	Bal.	0.22	0.53	1.44	0.025	0.022	0.038	–	–	
00Cr10MoV	Bal.	0.014	0.487	1.49	0.013	0.007	0.059	10.37	1.16	

Note: Bal. is the balance content.

content (< 3 wt%), the high corrosion resistance is primarily attributed to the formation of protective rust layer rather than the protective passive film [42,43,45,51–53].

In severe marine environment, Cr-bearing alloy steels may be applied together with AAS concrete to ensure a long service life. However, few researchers have addressed this issue and the passivation capability and corrosion behaviour of alloy steels in AAS concrete are still unclear. As a result, the aim of this work is to validate the electrochemical performance and corrosion morphology of a novel alloy steel in AAS and OPC mortars after long-term accelerated corrosion induced by chlorides. Conventional low-carbon steel was also evaluated for comparative purpose under the same condition.

2. Experimental

2.1. Materials

Two types of $\Phi 16$ reinforcing steels, namely, low-carbon steel (20MnSiV) and alloy steel (00Cr10MoV) manufactured in Shasteel Group were prepared. The chemical compositions of steels are shown in Table 1. The polished steels were etched to observe the cross-sectional microstructure using an optical microscope (Olympus, BHM), shown in Fig. 1. It can be seen in Fig. 1a that, 20MnSiV steel has a typical microstructure (brighter ferrite phase and darker pearlite phase) of conventional reinforcing steel in construction [54]. The brighter ferrite phase and darker bainite phase can be observed for 00Cr10MoV steel (Fig. 1b) [47].

Notably, both steels were embedded in mortar specimens in as-received condition (with mill scale) in order to reflect the real construction environments (Fig. 2). Fig. 3 shows the cross-sectional microstructure of the mill scale for uncorroded steels. 20MnSiV steel has a uniform and defective mill scale with the thickness of roughly $30\ \mu\text{m}$ (Fig. 3a) and the mill scale of 00Cr10MoV steel is more heterogeneous and much thinner (Fig. 3b). It should be mentioned in the elemental mappings (Fig. 3b) that Cr depletion in the mill scale could be observed for 00Cr10MoV steel, which is consistent with the previous reports [7,50].

The chemical compositions of P-II 42.5 R ordinary Portland cement (OPC) and ground granulated blast furnace slag (GGBFS) are shown in Table 2. River sand with the fineness modulus of 2.40 and tap water were used for the preparation of mortar specimens. The chemical

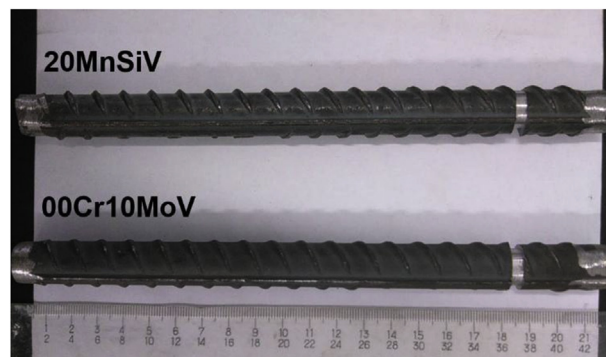


Fig. 2. The photographs of 20MnSiV and 00Cr10MoV steels both with mill scale.

composition of commercial sodium silicate solution used for AAS mortars is 29.58 wt% SiO_2 + 13.15 wt% Na_2O + 57.27 wt% H_2O .

2.2. Preparation of mortar specimens

The mixture proportion of OPC mortar is water/sand/cement = 0.6/3/1 (mass ratio), and the mixture proportion of AAS mortar is activator solution/sand/slag = 0.6/3/1 (mass ratio). The activator solution consists of a mixture of commercial sodium silicate solution, sodium hydroxide (analytical reagent) and deionized water with $\text{SiO}_2/\text{Na}_2\text{O}$ (mole ratio) of 1.2. The Na_2O concentration in the activator solution was 4% by weight of slag.

A schematic diagram of mortar specimen is shown in Fig. 4a. The mortar specimens had a 50 mm \times 50 mm cross-section and a length of 200 mm. Steel was embedded centrally in mortar specimen with the cover depth of 17 mm. A copper wire was soldered to one end of the reinforcing steel for electrochemical tests. In order to mitigate the crevice corrosion, the ends of steels were covered with insulating tape (inner layer) and epoxy coating (outer layer). Moreover, the edge of epoxy coating was sealed with adhesive sealant (Fig. 4a). The exposure length of steel is 10 cm and exposed surface area is approximately $50.3\ \text{cm}^2$ (Fig. 4a).

After casting, the ends of mortar specimens were coated with epoxy coating for avoiding the ingress of solutions from the ends. Thereafter, they were cured at standard curing room (temperature = $20 \pm 2\ ^\circ\text{C}$, and RH > 95%) for 28 days. Triplicate mortar specimens were prepared for each case to ensure the reproducibility of results.

At the same time, prismatic mortar specimens (40 mm \times 40 mm \times 160 mm) without steels were prepared for mechanical properties. Slightly higher flexural strength and compressive strength after 28 days of curing were recorded for AAS mortars compared with OPC mortars (Table 3).

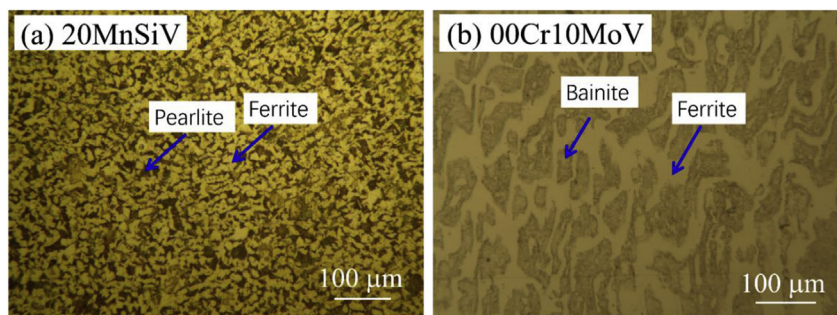


Fig. 1. Optical micrographs of 20MnSiV and 00Cr10MoV steels.

Download English Version:

<https://daneshyari.com/en/article/7883539>

Download Persian Version:

<https://daneshyari.com/article/7883539>

[Daneshyari.com](https://daneshyari.com)